Supporting Information

Nelson et al. 10.1073/pnas.1419264112

SI Text

Mutational Analysis of c-AMP-GMP Riboswitches. A number of differences between c-di-GMP-I riboswitches in Deltaproteobacteria and c-AMP-GMP riboswitches became apparent upon the construction of consensus sequences for each group. Apart from the prominent G20A deviation, c-AMP-GMP riboswitches also contain additional unpaired nucleotides in the P3 stem, a semiconserved internal loop in the P1 stem, and additional conserved nucleotides in the ligand-binding pocket (Fig. 2*B*). Given that mutation of position 20 in a c-AMP-GMP back to guanosine is not sufficient to completely convert the RNA ligand specificity to c-di-GMP (Fig. S3), we hypothesized that one or more of these additional changes might contribute to c-AMP-GMP selectivity. Mutation of each of these positions singly failed to convert the RNA to a c-di-GMP selective aptamer (Fig. S5). However, concomitant mutation of position 20 and disruption of the loop within the P1 stem (M8) produced an aptamer with a modest preference for c-di-GMP (Fig. S5), suggesting that these nucleotides might be important in tuning selectivity. Furthermore, these data suggest that examination of other putative c-di-GMP-I riboswitches with alterations in the P1 stem might be another strategy for identifying additional cyclic dinucleotide riboswitch classes.

Signaling by c-AMP-GMP and Exoelectrogenesis. One of the challenges of studying electrogenesis in *Geobacter* spp. is the determination of which of the numerous different cytochrome *c* proteins in these organisms are involved in the reduction of extracellular metals (1). We have identified approximately 25 cytochrome *c* genes in various *Geobacter* spp. controlled by c-AMP-GMP that we suspect constitute a large portion of these genes. Also, we note the presence of several genes involved in aromatic amino acid biosynthesis controlled by riboswitches in *Geobacter* spp. (Fig. 3*A* and Fig. S6). Aromatic amino acids have been invoked as a mechanism to confer a metal-like conductivity to PilA in *Geobacter* (2), although this explanation has been disputed (3). The control of such genes by c-AMP-GMP suggests that they are important for exoelectrogenesis in some fashion.

Intriguingly, *G. metallireducens* has been shown to access insoluble Fe(III) oxide via chemotaxis, triggered via an unknown mechanism (4). Chemotaxis has also been proposed to be at least partially under the control of c-AMP-GMP in *V. cholerae* (5), suggesting that the same may be true here. The *pilMNOPQ* operon is frequently controlled by c-AMP-GMP riboswitches in *Geobacter* spp. (Fig. 3 and Fig. S6). This operon constitutes a type IV pilin secretion system that is important for twitching motility in other Proteobacteria and is known to interact with the type IV pilin PilA (6), which is critical for motility and exoelectrogenesis in *Geobacter* spp. (4, 7). However, twitching motility itself does not appear important for iron oxide reduction in *G. sulfurreducens* (8), and we do not observe a significant number of genes predicted to be involved in chemotaxis controlled by c-AMP-GMP riboswitches. However, a number of predicted c-di-GMP phosphodiesterases and synthases are found downstream of c-AMP-GMP riboswitches. In many organisms, chemotaxis is controlled by c-di-GMP-responsive riboswitches (9, 10). For all such RNAs examined to date, decreasing c-di-GMP concentrations are predicted to trigger chemotaxis. In *Geobacter* spp., the degradation of c-di-GMP could be controlled by c-AMP-GMP via these phosphodiestereases, which could serve as a potential mechanism whereby c-AMP-GMP could indirectly control chemotaxis.

Possible Roles for Genes Controlled by c-AMP-GMP in Exoelectrogenesis. Many of the genes controlled by c-AMP-GMP riboswitches might be important targets for engineering *Geobacter* strains with improved energy production or bioremediation properties (11–14). For example, fibronectin domains are commonly controlled by the riboswitch but have not been specifically implicated in any exoelectrogenic process. These proteins could be involved in the adherence of bacteria to insoluble iron oxide particles (15), actually be cytochromes themselves (16), or be involved in both adherence and electron transfer. Additionally, genes downstream of c-AMP-GMP riboswitches involved in peptidoglycan remodeling could play a role in the synthesis or remodeling of extracellular polysaccharide networks important for exoelectrogenesis in *Geobacter* (17, 18).

Notably, we also observed a small number of cytochrome *c* type genes controlled by c-di-GMP-I riboswitches, suggesting that c-di-GMP also plays a role in these same processes. It is known that different electrogenesis pathways in *Geobacter* spp. are expressed when the bacteria are in biofilms compared with growth on iron oxide (19). We speculate that c-AMP-GMP and c-di-GMP might control these different pathways. For example, c-AMP-GMP could activate chemotaxis and the initial stages of adherence in the presence of a potential insoluble reducing agent, analogous to the colonization of *V. cholerae* in a host organism. Then, during formation of a biofilm around the metal ion complex, c-di-GMP could activate a separate electrogenesis pathway. Indeed, differences in the ability of *G. sulfurreducens* to produce an electric current have been observed in early adherence to electrodes compared with biofilms (20).

Riboswitches that sense c-AMP-GMP are also found in other Deltaproteobacteria. For example, a gene predicted to encode coenzyme F_{390} synthetase (*paaK*) appears downstream of a c-AMP-GMP riboswitch in *Pelobacter carbinolicus*. Interestingly, coenzyme F_{390} has been suggested to function as a redox sensor in various methanogenic archaea and might be involved in similar processes here (21). Notably, we do not observe c-AMP-GMP riboswitches in *Shewanella* or *Geothrix* species, which appear to use electron shuttles rather than conductive pili for the reduction of iron oxide (22, 23), suggesting that the association of c-AMP-GMP with this process may be due more to the need to adhere to insoluble iron oxide than to the utilization of extracellular electron acceptors.

Searching for Additional Riboswitch Variants. When attempting to identify additional riboswitch classes that recognize other cyclic dinucleotides, we first examined riboswitches that contained deviations from the c-di-GMP-I consensus. Whereas G20A is the most common of these, differences are also occasionally observed at the C92 position. Additionally, a few predicted riboswitches can be identified that contain G20U or G20C mutations. Finally, certain riboswitches control genes somewhat distinct from those typical of c-di-GMP-I riboswitches (such as several in Betaproteobacteria that control the expression of spherulins). We regarded all of these RNAs as potential candidates for testing with alternative cyclic dinucleotides. However, upon testing, we observed maintenance of c-di-GMP binding, obvious misfolding of the RNA constructs, or a complete lack of recognition for any ligand tested. Below we note a few interesting findings that we observed over the course of this work.

Riboswitches for c-di-GMP, c-di-AMP, and c-AMP-GMP have now been identified. However, one additional cyclic dinucleotide has been reported. This molecule (c-GAMP) consists of one GMP

and one AMP moiety linked via one 3′-5′ and one 2′-5′ phosphodiester linkage and has been found only in metazoans to date (24–28). All of the RNAs that we studied were examined for their ability to recognize this cyclic dinucleotide, but we did not observe any modulation of RNA structure for any aptamer with physiologically relevant concentrations of c-GAMP.

Another riboswitch aptamer was tested for c-GAMP affinity because of its proximity to various CRISPR motifs (29). This RNA has only a minimal affinity for c-di-GMP, likely due to the lack of any P1 stem for this riboswitch aptamer, an unusual occurrence for which there are several possible explanations. First, this construct might represent a degenerate riboswitch in the process of being eliminated from the genome. Second, it might control CRISPR expression under thermodynamic, rather than kinetic, control. Some riboswitches operate under kinetic control (30), necessitating binding affinities substantially better than the actual ligand concentration in the cell. If this RNA maintains the ability to regulate gene expression, the mechanism by which it does so could be highly unusual, especially as it is found near CRISPR motifs. Third, this RNA might originate in clostridial phage and have been captured by CRISPR sometime in the past. It does bear significant identity to c-di-GMP-I RNAs known in phage. However, the RNA is roughly 100 nucleotides in size, which is roughly an order of magnitude larger than known CRIPSR inserts.

Finally, we also examined a second class of c-di-GMP riboswitches, called c-di-GMP-II, with changes in either gene association or nucleotide identity within the ligand-binding pocket for any potential switch in specificity. We noted RNAs upstream of genes annotated as being involved in sporulation, as well as RNAs that differed significantly in their binding pocket. However, upon examination, none of these RNAs had any change in specificity observed relative to canonical c-di-GMP-II riboswitches.

Thus, we have not yet identified any additional second messenger-sensing riboswitch variants with alternative ligand specificity. However, it is important to note that these results should not be taken as evidence that such riboswitches do not exist. The recent discovery of c-AMP-GMP itself suggests the possibility that more such signaling molecules might yet exist and, with their identification, we may be able to again identify a corresponding riboswitch-controlled superregulon. For example, we found that, under our conditions, 128 *GGDEF* RNA from *Paenibacillus mucillaginosus* requires high concentrations of c-di-GMP or c-AMP-GMP to exhibit binding (Fig. 2). This unusually poor affinity and selectivity for these second messengers could be due to a poor choice of RNA constructs for testing, could reflect a naturally poor affinity for its biologically relevant ligand, or could indicate that an undiscovered natural analog of c-AMP-GMP and c-di-GMP is the true ligand.

1. Methé BA, et al. (2003) Genome of *Geobacter sulfurreducens*: Metal reduction in subsurface environments. *Science* 302(5652):1967–1969.
2. Vargas M, et al. (2013) Aromatic amino acids required for pili conductivity and long-range extracellular electron transport in *Geobacter sulfurreducens*. *MBio* 4(2):e00105–e00113.
3. Snider RM, Strycharz-Glaven SM, Tsoi SD, Erickson JS, Tender LM (2012) Long-range electron transport in *Geobacter sulfurreducens* biofilms is redox gradient-driven. *Proc Natl Acad Sci USA* 109(38):15467–15472.
4. Childers SE, Ciufo S, Lovley DR (2002) *Geobacter metallireducens* accesses insoluble Fe(III) oxide by chemotaxis. *Nature* 416(6882):767–769.
5. Davies BW, Bogard RW, Young TS, Mekalanos JJ (2012) Coordinated regulation of accessory genetic elements produces cyclic di-nucleotides for *V. cholerae* virulence. *Cell* 149(2):358–370.
6. Tammam S, et al. (2013) PilMNOPQ from the Pseudomonas aeruginosa type IV pilus system form a transenvelope protein interaction network that interacts with PilA. *J Bacteriol* 195(10):2126–2135.
7. Richter LV, Sandler SJ, Weis RM (2012) Two isoforms of *Geobacter sulfurreducens* PilA have distinct roles in pilus biogenesis, cytochrome localization, extracellular electron transfer, and biofilm formation. *J Bacteriol* 194(10):2551–2563.
8. Reguera G, et al. (2005) Extracellular electron transfer via microbial nanowires. *Nature* 435(7045):1098–1101.
9. Sudarsan N, et al. (2008) Riboswitches in eubacteria sense the second messenger cyclic di-GMP. *Science* 321(5887):411–413.
10. Lee ER, Baker JL, Weinberg Z, Sudarsan N, Breaker RR (2010) An allosteric self-splicing ribozyme triggered by a bacterial second messenger. *Science* 329(5993):845–848.
11. Lovley DR (2001) Bioremediation. Anaerobes to the rescue. *Science* 293(5534): 1444–1446.
12. Cologgi DL, Lampa-Pastirk S, Speers AM, Kelly SD, Reguera G (2011) Extracellular reduction of uranium via *Geobacter* conductive pili as a protective cellular mechanism. *Proc Natl Acad Sci USA* 108(37):15248–15252.
13. Lovley DR (2006) Bug juice: Harvesting electricity with microorganisms. *Nat Rev Microbiol* 4(7):497–508.
14. Lovley DR (2006) Microbial fuel cells: Novel microbial physiologies and engineering approaches. *Curr Opin Biotechnol* 17(3):327–332.
15. Kataeva IA, et al. (2002) The fibronectin type 3-like repeat from the Clostridium thermocellum cellobiohydrolase CbhA promotes hydrolysis of cellulose by modifying its surface. *Appl Environ Microbiol* 68(9):4292–4300.
16. Martinez SE, Huang D, Szczepaniak A, Cramer WA, Smith JL (1994) Crystal structure of chloroplast cytochrome f reveals a novel cytochrome fold and unexpected heme ligation. *Structure* 2(2):95–105.
17. Rollefson JB, Levar CE, Bond DR (2009) Identification of genes involved in biofilm formation and respiration via mini-Himar transposon mutagenesis of *Geobacter sulfurreducens*. *J Bacteriol* 191(13):4207–4217.
18. Rollefson JB, Stephen CS, Tien M, Bond DR (2011) Identification of an extracellular polysaccharide network essential for cytochrome anchoring and biofilm formation in *Geobacter sulfurreducens*. *J Bacteriol* 193(5):1023–1033.
19. Kato S, Hashimoto K, Watanabe K (2013) Iron-oxide minerals affect extracellular electron-transfer paths of *Geobacter* spp. *Microbes Environ* 28(1):141–148.
20. Marsili E, Sun J, Bond DR (2010) Voltammetry and growth physiology of *Geobacter sulfurreducens* biofilms as a function of growth stage and imposed electrode potential. *Electroanalysis* 22(7-8):865–874.
21. Vermeij P, van der Steen RJT, Keltjens JT, Vogels GD, Leisinger T (1996) Coenzyme F390 synthetase from *Methanobacterium thermoautotrophicum* Marburg belongs to the superfamily of adenylate-forming enzymes. *J Bacteriol* 178(2):505–510.
22. Newman DK, Kolter R (2000) A role for excreted quinones in extracellular electron transfer. *Nature* 405(6782):94–97.
23. Nevin KP, Lovley DR (2002) Mechanisms for accessing insoluble Fe(III) oxide during dissimilatory Fe(III) reduction by *Geothrix fermentans*. *Appl Environ Microbiol* 68(5): 2294–2299.
24. Zhang X, et al. (2013) Cyclic GMP-AMP containing mixed phosphodiester linkages is an endogenous high-affinity ligand for STING. *Mol Cell* 51(2):226–235.
25. Gao P, et al. (2013) Cyclic [G(2′,5′)pA(3′,5′)p] is the metazoan second messenger produced by DNA-activated cyclic GMP-AMP synthase. *Cell* 153(5):1094–1107.
26. Diner EJ, et al. (2013) The innate immune DNA sensor cGAS produces a noncanonical cyclic dinucleotide that activates human STING. *Cell Reports* 3(5):1355–1361.
27. Sun L, Wu J, Du F, Chen X, Chen ZJ (2013) Cyclic GMP-AMP synthase is a cytosolic DNA sensor that activates the type I interferon pathway. *Science* 339(6121):786–791.
28. Wu J, et al. (2013) Cyclic GMP-AMP is an endogenous second messenger in innate immune signaling by cytosolic DNA. *Science* 339(6121):826–830.
29. Sorek R, Lawrence CM, Wiedenheft B (2013) CRISPR-mediated adaptive immune systems in bacteria and archaea. *Annu Rev Biochem* 82:237–266.
30. Nelson JW, et al. (2013) Riboswitches in eubacteria sense the second messenger c-di-AMP. *Nat Chem Biol* 9(12):834–839.

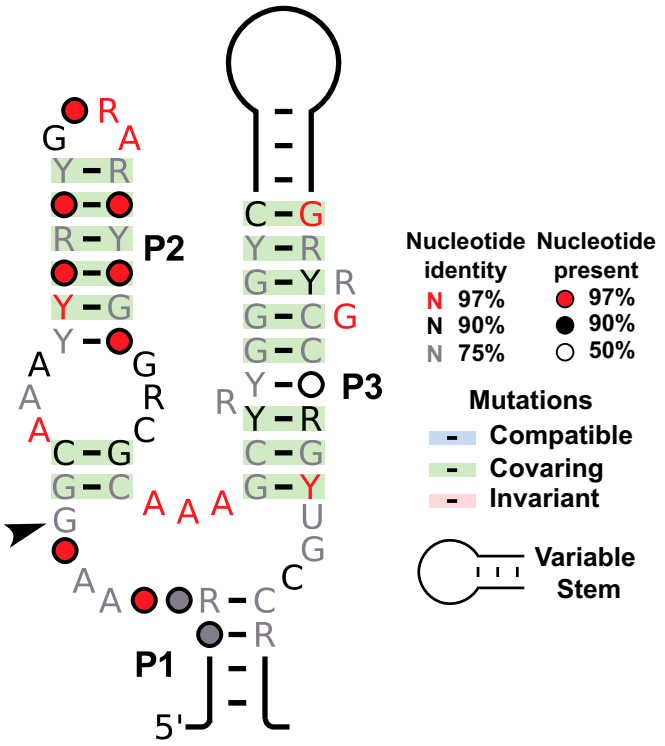

Fig. S1. Consensus sequence and secondary structure of GEMM motif RNAs. The consensus is based on 6,800 examples from sequenced bacterial species and from environmental sequences. The P1 stem is not well conserved and is therefore difficult to predict precisely. Consequently, it is shown as a variable length stem of uncertain length. Additional annotations are as described in the legend for Fig. 2*B*.

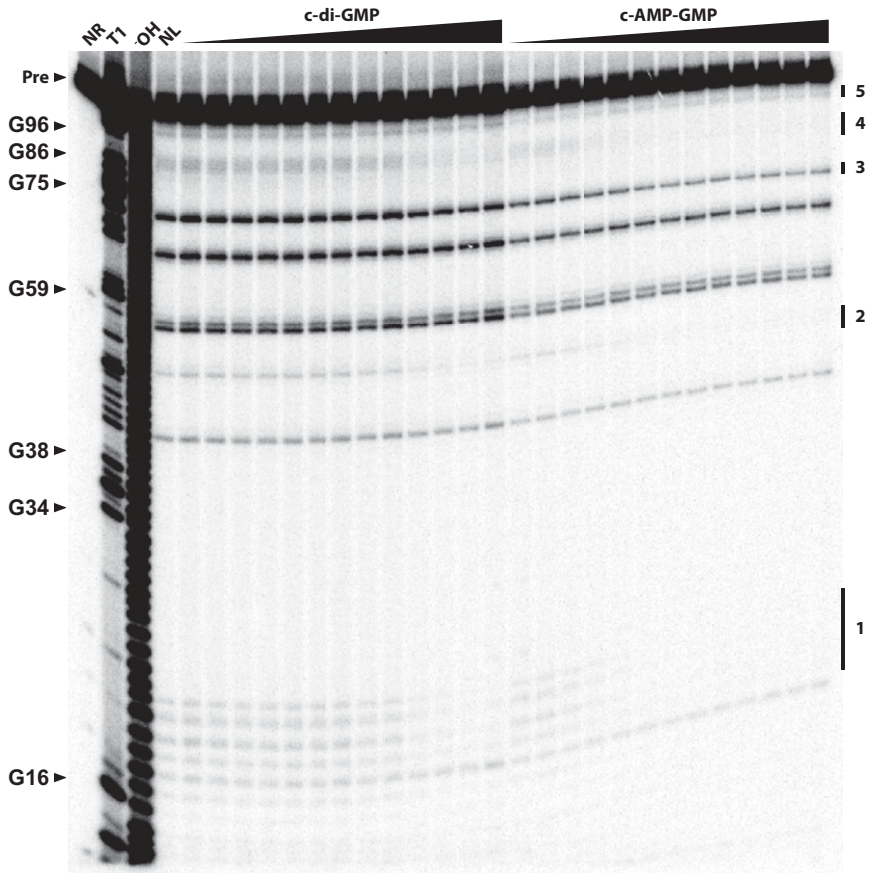

Fig. S2. PAGE analysis of in-line probing of 5′ ^{32}P-labeled 100 *erfK* RNA in the presence of increasing c-di-GMP or c-AMP-GMP. Annotations are as described in the legend for Fig. 1*C*. Concentrations of ligands used range from 100 pM to 10 μM in half-log unit increments, or the sample was incubated in the absence of ligand (–). Data from this gel are quantified and presented in Fig. 1*D*.

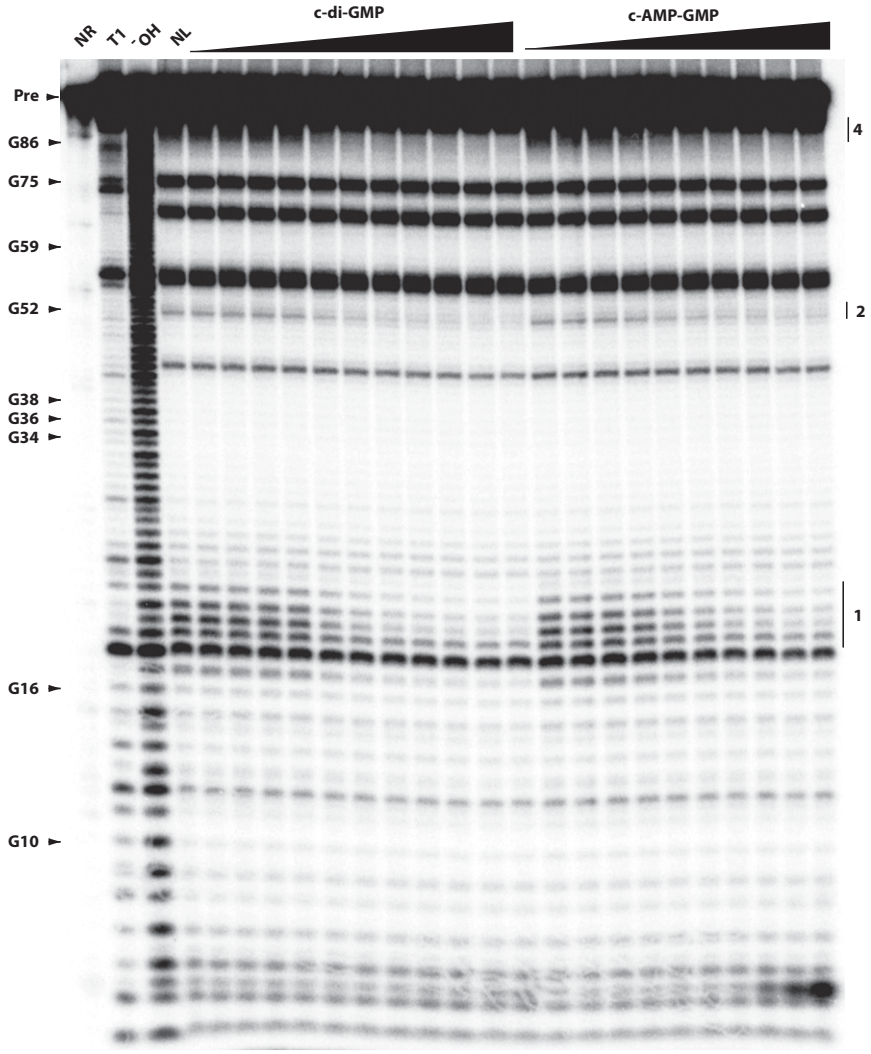

Fig. S3. PAGE analysis of in-line probing of 100 *erfK* M1 in the presence of increasing c-AMP-GMP and c-di-GMP. The sequence of the M1 construct is presented in Fig. 1*B*. Annotations are as described in the legend for Fig. 1*C*. Ligand concentrations range from 10 pM to 10 μM in half-log unit increments. Data from this figure were used to determine the dissociation constants presented for 100 *erfK* M1 in Fig. S5.

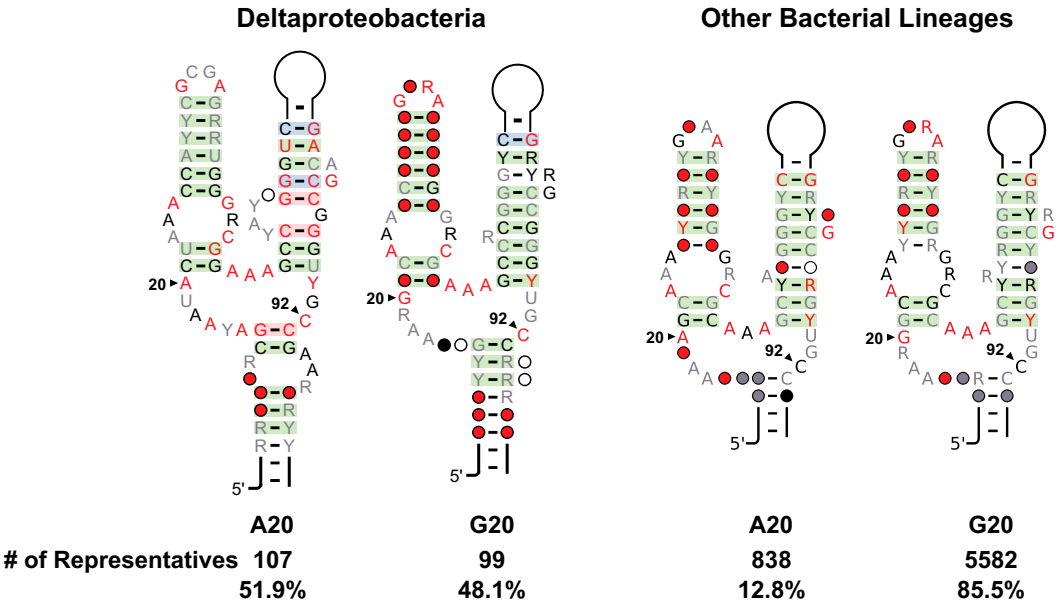

Fig. S4. Percentage of GEMM motif RNAs containing G or A at position 20 in Deltaproteobacteria versus all other bacterial lineages. Annotations are as described in the legend for Fig. 2*B*.

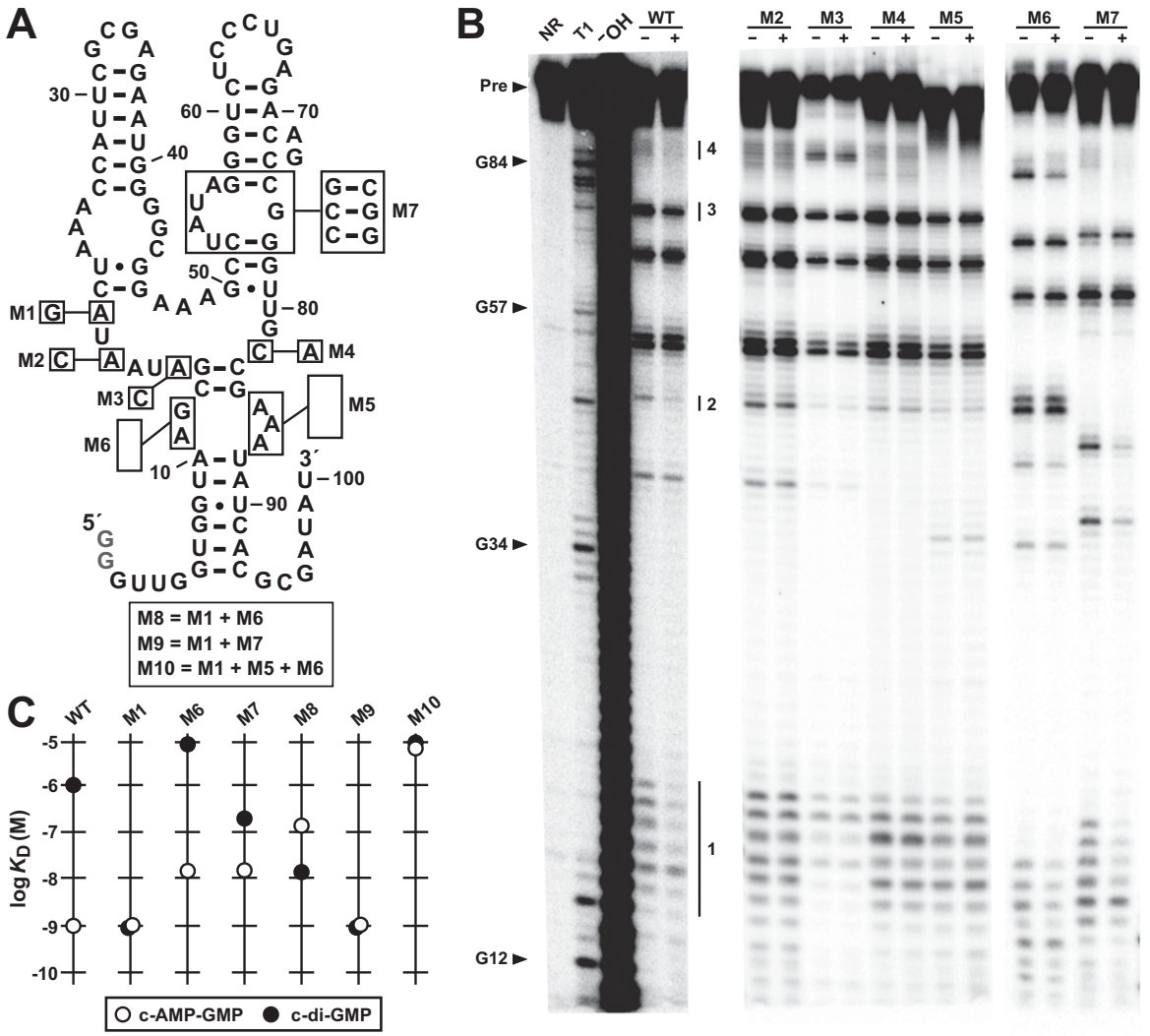

Fig. S5. Ligand binding by RNAs mutated at positions conserved by c-AMP-GMP riboswitches but not by c-di-GMP-I riboswitches. (*A*) Sequence and secondary structure of the 100 *erfK* riboswitch aptamer from *G. metallireducens* and various mutant constructs. Annotations are as described in the legend for Fig. 1*B*. Note that M5 and M6 are deletions of the boxed nucleotides. (*B*) PAGE analysis of in-line probing assay reactions with 100 *erfK* riboswitch aptamer (WT) and mutants M2–M7 incubated in the absence (–) or presence (+) of 10 μM c-AMP-GMP. No evidence of binding is observed for M2–M5. Annotations are as described in the legend for Fig. 1C. (*C*) Plot of the logarithm of K_D values for c-di-GMP and c-AMP-GMP, the WT 100 *erfK* riboswitch aptamer (WT), mutants M1 (using the data from Figs. S2 and S3), M6, M7, and combined mutants represented by M8, M9, and M10. K_D values were derived by quantifying the modulation of spontaneous cleavage products generated by in-line probing reactions as depicted in Fig. 1*D*.

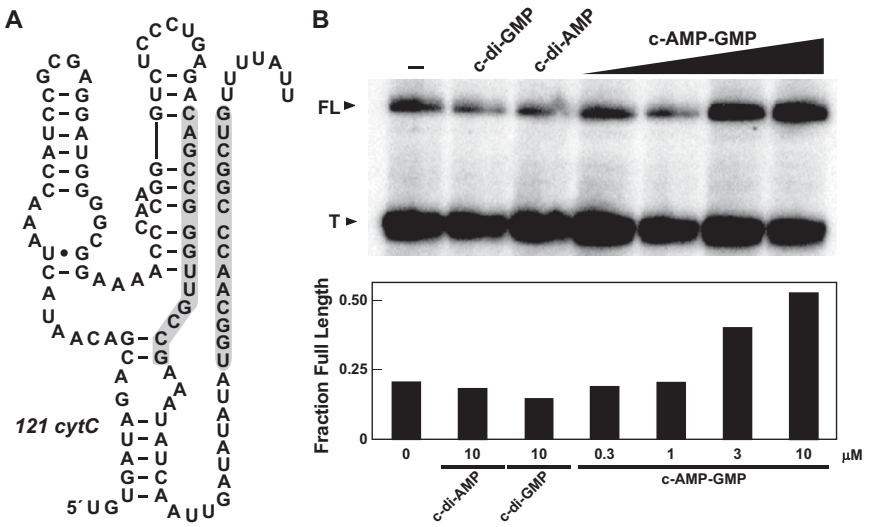

Fig. S6. Single-round in vitro transcription of a c-AMP-GMP riboswitch. (*A*) Schematic representation of the *cytC* riboswitch and gene association from *G. metallireducens* in the presence of c-AMP-GMP. The predicted terminator stem is highlighted in gray. (*B*, *Upper*) PAGE analysis of single-round in vitro transcription reactions using a DNA template for the riboswitch in *A*. Transcription reactions (*Materials and Methods*) are conducted in the absence (–) or presence of various cyclic dinucleotides at the indicated concentrations. Predicted full-length and terminated products are designated by FL and T. (*B*, *Lower*) Plot of the fraction of full-length RNA transcripts produced as determined from the PAGE data (*Upper*).

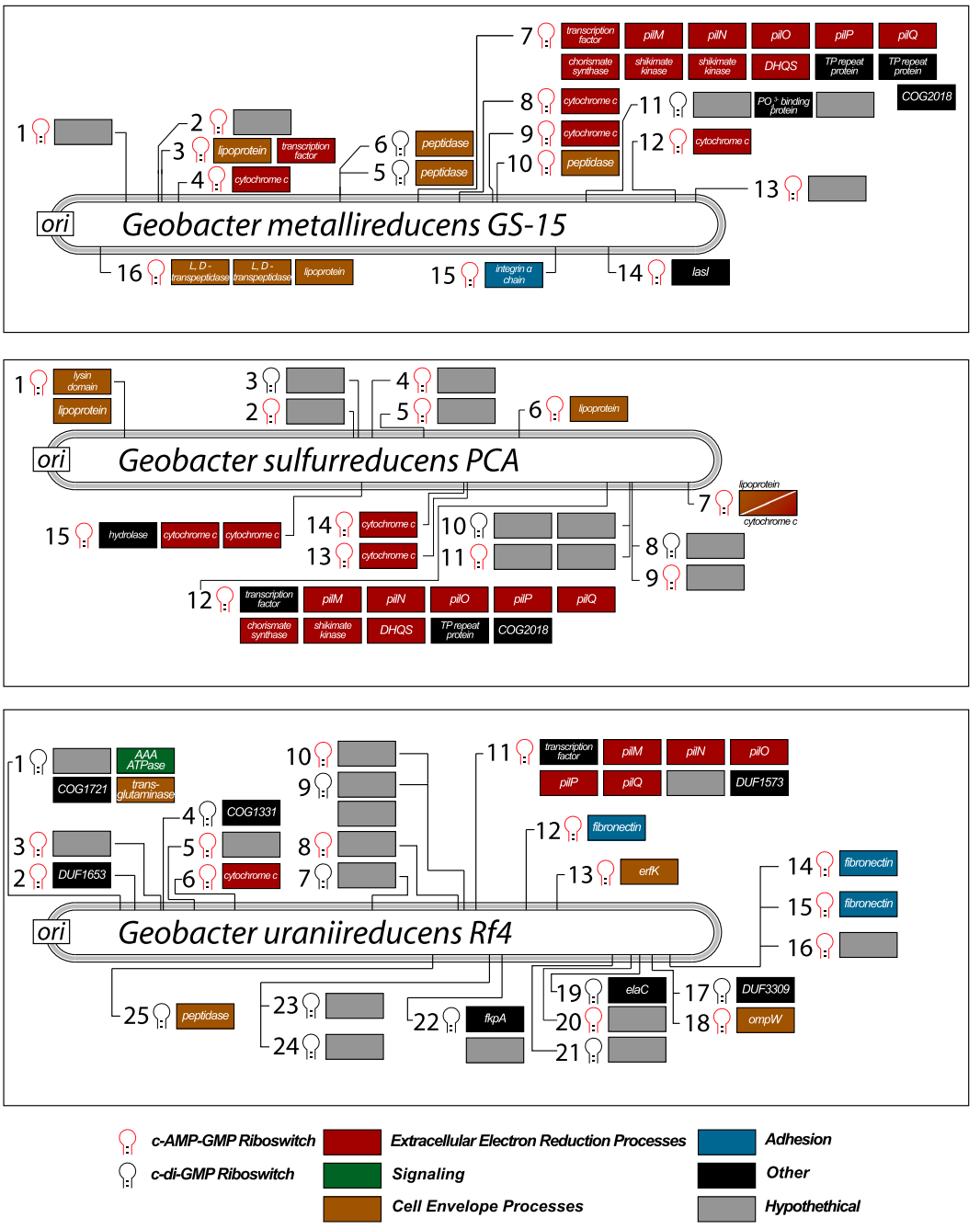

Fig. S7. Genes downstream of c-di-GMP and c-AMP-GMP riboswitches in selected species of *Geobacter* important for alternative energy production or bioremediation. No distinction is made between single and tandem riboswitch aptamers.

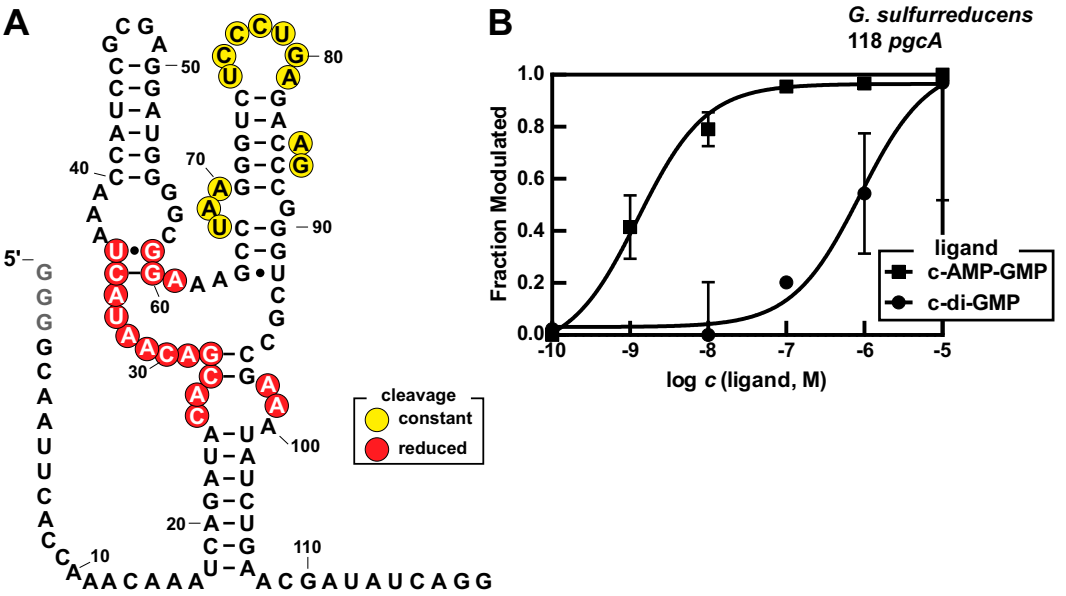

Fig. S8. Binding of c-AMP-GMP and c-di-GMP by *G. sulfurreducens* 118 *pgcA* RNA. (*A*) Sequence and secondary structure model of the 118 *pgcA* construct. Annotations are as described in the legend to Fig. 1*B*. (*B*) Plot of the fraction of riboswitch RNA bound to ligand versus the logarithm of the molar concentration of ligand, as inferred from in-line probing assay data. Data points are the average of the normalized fraction of RNA cleavage at multiple sites, and error bars represent the SD.

Other Supporting Information Files

Table S1 (DOCX)
Table S2 (DOCX)
Table S3 (DOCX)
Dataset S1 (PDF)